with iatrogenic, congenital, or acquired immunodeficiency can reveal an increased number of EBV-infected cells in the lymph nodes.[4] EBV is also associated with various malignant lymphomas and lymphoproliferative disorders.

Only 1 case of IgG4-related lymphadenopathy with EBV-infected cells has been reported, and the relationship between IgG4-related disease and EBV has not been fully addressed.[5] Hence, we analyzed the association of EBV and IgG4-related disease. Lymph node tissues from subjects with various morphologic types of IgG4-related lymphadenopathy were subjected to EBER in situ hybridization (ISH) to examine the presence and localization of $EBER^+$ cells. For comparison with extranodal lesions, IgG4-related lacrimal gland disease, IgG4-related submandibular gland disease, IgG4-related skin disease, and IgG4-related pancreatitis were also examined. Non–IgG4-related benign lymph node hyperplasia and lymph nodes of AITL were also examined for comparison.

MATERIALS AND METHODS

Patients and Materials

Thirty-one Japanese patients with IgG4-related lymphadenopathy, 9 with IgG4-related lacrimal gland disease, 10 with IgG4-related submandibular disease, 2 with IgG4-related skin disease, 3 with IgG4-related pancreatitis, 22 with $IgG4^-$ reactive lymphoid hyperplasia, and 10 with AITL were included. All cases were retrieved from the surgical pathology consultation files of the Department of Pathology, Graduate School of Medicine, Dentistry, and Pharmaceutical Sciences, Okayama University in Okayama, Japan.

The diagnoses of IgG4-related disease were based upon the consensus statement on the pathology of IgG4-related disease published in 2012.[6] The clinical records and pathology materials of all IgG4-related diseases were reviewed, and cases of multicentric Castleman disease, malignant lymphoma, or other lymphoproliferative disorders (including rheumatoid arthritis–related lymphadenopathy and other immune-mediated conditions) were excluded. The number of $IgG4^+$ cells in the cases of IgG4-related lymphadenopathy ranged from 122 to 477 per high-power field (HPF) (mean ± SD, 250 ± 102). The ratio of $IgG4^+/IgG^+$ cells was >0.4 in all cases. The specimens of IgG4-related lymphadenopathy were reviewed by the authors Y.S. and M.T. and morphologically categorized into the following subtypes as previously reported[1,7]: Castleman disease–like morphology (type I); reactive follicular hyperplasia (type II); interfollicular expansion and increased immunoblasts (type III); PTGC-type (type IV); and inflammatory pseudotumor-like morphology (type V).

In sections of IgG4-related lacrimal gland disease, IgG4-related submandibular gland disease, IgG4-related skin disease, and IgG4-related pancreatitis, characteristic morphologic features and increased $IgG4^+$ cells were seen. Only in cases of IgG4-related skin diseases, the required numbers of $IgG4^+$ plasma cells were not seen; however, in a previous study of IgG4-related skin disease, we suggested that the cutoff of 200 $IgG4^+$ plasma cells/HPF appeared to be controversial.[8] Two patients with IgG4-related lacrimal gland disease (cases Ex4 and Ex7) were the same patients with IgG4-related lymphadenopathy listed in Table 1 (cases LN6 and LN25, respectively).

To examine whether increased numbers of EBV-infected cells in benign lymph nodes was specifically associated with IgG4-related disease rather than other patient characteristics, EBER detection by ISH was also performed on 22 lymph nodes with $IgG4^-$ lymphoid hyperplasia. The cases of reactive lymphoid hyperplasia did not suggest Castleman disease or any other distinct lymphoproliferative diseases and also did not meet the histologic diagnostic criteria for IgG4-related disease.

To compare with type III IgG4-related lymphadenopathy, immunostaining for IgG4 was performed in 10 lymph nodes with AITL. Cases of AITL were diagnosed on the basis of *World Health Organization (WHO) Classification of Tumours of Haematopoietic and Lymphoid Tissues* (fourth edition).[9] All cases showed typical histologic features including infiltration of small to medium-sized T cells with clear cytoplasm and proliferation of high endothelial venules. Many $EBER^+$ B cells (from 23 to $>1000/0.5\,cm^2$; mean ± SD 422 ± 399) were observed in 8 of 10 cases (80%), which is similar to the percentage described in the WHO monograph (75%).[9]

Histologic Examination and Immunohistochemistry

Surgically biopsied lymph node specimens were fixed in 10% formaldehyde and embedded in paraffin. Serial sections (4 μm) were cut from each paraffin-embedded tissue block, and stained with hematoxylin and eosin. An automated Bond Max stainer (Leica Biosystems, Melbourne, Vic., Australia) was used for immunohistochemistry. The tissue sections were subjected to standard heating or enzymatic pretreatment for antigen retrieval. The following primary antibodies were used: IgG (polyclonal; 1:20,000; Dako, Carpinteria, CA), IgG4 (HP6025; 1:400; The Binding Site, Birmingham, UK), FOXP3 (236A/E7; 1:100; Abcam, Cambridge, UK), and latent membrane protein-1 (LMP-1) (CS1-CS4; 1:10; Novocastra).

On the basis of the consensus statement on the pathology of IgG4-related disease,[6] 3 different HPFs (eyepiece, ×10; lens, ×40) were examined to calculate the average number of $IgG4^+$ cells per HPF and the $IgG4^+/IgG^+$ cell ratio. $FOXP3^+$ cells were also counted at 3 different HPFs with the highest density to calculate the average numbers per HPF.

In Situ Hybridization

ISH of EBER was performed using an automated Bond Max stainer (Leica Biosystems). Three representative fields per case were captured using a ×4 objective lens (covering $0.167\,cm^2$) to count $EBER^+$ cells per $0.5\,cm^2$. Increased numbers of EBV^+ cells was defined as >10 $EBER^+$ cells/$0.5\,cm^2$.[10] EBER-ISH^+ and $LMP\text{-}1^-$ cases were classified into EBV latency type I.

TABLE 1. Clinical Features of 31 Patients of IgG4-related Lymphadenopathy

No.	Age/Sex	Affected Lymph Nodes	Extranodal Sites	IgG4 (mg/dL; nl = 4.8-105)	IgG (mg/dL)	IgG4/IgG (%; nl = 3-6)
LN1	58/M	Cervix, supraclavicle, axilla, mediastinum, porta hepatis, lesser omentum		2010	3536	57
LN2	74/M	Cervix, para-aorta, parailiac artery	Submandibular gland	NA	4050	NA
LN3	59/M	Cervix, supraclavicle, axilla, mediastinum, inguen		1140	5257	22
LN4	64/F	Left cervix, mediastinum		446	1989	22
LN5	82/F	Right auricular, supraclavicle	Salivary gland	327	1094	30
LN6*	36/F	Cervix, supraclavicle	Lacrimal gland	561	1961	29
LN7	64/M	Mediastinum, axilla	Right lung	641	3134	20
LN8	77/M	Systemic		1100	5800	19
LN9	78/M	Mediastinum, axilla, inguen		1090	5174	21
LN10	82/M	Cervix, inguen, para-aorta, mediastinum	Parotid gland, lacrimal gland	1050	3447	30
LN11	68/F	Axilla, mediastinum, abdomen, inguen		2120	5057	42
LN12	67/M	Cervix, mediastinum, axilla, para-aorta		583	2468	24
LN13	76/M	Cervix, axilla, para-aorta, inguen		1040	3930	26
LN14	59/F	Supraclavicle, mediastinum, abdomen, inguen	Lacrimal gland, submandibular gland	1500	2524	59
LN15	73/M	Abdomen, inguen	Kidney	505	1600	32
LN16	36/M	Left submandibulla		110	551	20
LN17	69/M	Right submandibulla		693	2315	30
LN18	71/M	Left submandibulla, submentum		275	2144	13
LN19	50/M	Bilateral submandibulla, cervix		183	2719	7
LN20	61/M	Systemic	Skin	1120	3025	37
LN21	51/F	Right submandibulla	Bilateral eyelid, parotid gland	223	NA	NA
LN22	70/M	Cervix	Bilateral parotid gland, right submandibular gland, pancreas	483	1190	41
LN23	67/M	Left submandibulla	Left submandibular gland	141	1543	9
LN24	67/M	Submandibulla	Right lung	389	1619	24
LN25†	68/M	Bilateral submandibulla	Bilateral lacrimal glands	1340	3090	43
LN26	63/M	Left submandibulla	Submandibular gland, kidney, mediastinum, aorta	2240	3007	74
LN27	65M	Right submandibulla, mediastinum	Bilateral lacrimal glands, submandibular gland, parotid gland, kidney	2550	6024	42
LN28	70M		Lung	236	1466	16
LN29	51F	Right submandibulla	Submandibular gland	NA	NA	NA
LN30	76M	Right submandibulla	Lacrimal gland, skin	NA	NA	NA
LN31	49M	Left submandibulla, cervix	Left submandibular gland	NA	NA	NA

*The same patient had IgG4-related lacrimal gland disease listed in Table 4 (Ex4).
†The same patient had IgG4-related lacrimal gland disease listed in Table 4 (Ex7).
F indicates female; LN, lymph node; M, male; NA; not available; nl; normal.

Polymerase Chain Reaction for Immunoglobulin Heavy Chain and T-cell Receptor γ Chain

DNA was extracted from formalin-fixed and paraffin-embedded tissues. T-cell receptor γ chain (TCRG) VgIf and Vg10 primers (tube A) and TCRG Vg9 and Vg11 primers (tube B) were used for TCR gene rearrangement study, and each of the tubes (A and B) also included 2 primers targeting the J segments (Jg1.1/2.1 and Jg1.3/Jg2.3) as previously reported.[11] Polymerase chain reaction (PCR) for immunoglobulin heavy chain (IgH) was also performed using consensus primers directed to VH framework (FR) II of the IgH gene using BIOMED-2 primer sets as previously described.[11] The products of PCR reactions were subsequently analyzed by ABI PRISM 310 Genetic Analyzer and Gene Mapper software version 3.7 (Applied Biosystems, CA).[12]

Statistical Analysis

Differences between groups were determined by the Student t test and χ^2 test with SPSS software (version 14.0; SPSS Inc., Chicago, IL). Values of $P < 0.05$ was considered to be statistically significant.

RESULTS

IgG4-related Lymphadenopathy

The clinical and pathologic findings for 31 cases of IgG4-related lymphadenopathy are summarized

TABLE 2. Pathologic Features of 31 Patients of IgG4-related Lymphadenopathy

No.	Histologic Subtype	EBER-ISH$^+$ Cells (/0.5 cm^2)	Distribution of EBER$^+$ Cells
LN1	Type I	0	
LN2	Type I	48	Interfollicular/scattered
LN3	Type I	27	Interfollicular/scattered
LN4	Type II	0	
LN5	Type II	3	
LN6	Type II	13	Interfollicular/scattered
LN7	Type II	25	Interfollicular/scattered
LN8	Type III	3	
LN9	Type III	0	
LN10	Type III	0	
LN11	Type III	163	Interfollicular/scattered
LN12	Type III	> 1000	Diffuse
LN13	Type III	> 1000	Diffuse
LN14	Type III	133	Interfollicular/scattered
LN15	Type III	52	Interfollicular/scattered
LN16	Type IV	0	
LN17	Type IV	1	
LN18	Type IV	0	
LN19	Type IV	9	
LN20	Type IV	10	
LN21	Type IV	6	
LN22	Type IV	6	
LN23	Type IV	19	Interfollicular/scattered
LN24	Type IV	12	Interfollicular/scattered
LN25	Type IV	248	Intrafollicular/localized
LN26	Type IV	72	Interfollicular/scattered
LN27	Type IV	46	Interfollicular/scattered
LN28	Type IV	27	Interfollicular/scattered
LN29	Type IV	20	Interfollicular/scattered
LN30	Type IV	55	Interfollicular/scattered
LN31	Type IV	27	Interfollicular/scattered

in Tables 1 and 2. There were 24 men and 7 women. The ages ranged from 36 to 82 years (mean ± SD, 64.5 ± 11.6). No patient had a record of congenital, iatrogenic, or acquired immunodeficiency. There was no evidence of acute infection of EBV, and EBV serology indicated past infection in all patients tested. Serum IgG4 levels were elevated in all 27 examined patients and ranged from 110 to 2550 mg/dL (mean ± SD, 869.0 ± 695.3). Twenty-seven patients had systemic or multifocal lymphadenopathy, whereas 4 cases of PTGC-type (type IV) IgG4-related lymphadenopathy were localized in the submandibular lymph nodes (cases LN16 to LN19).

Histologically, cases were classified into type I (n = 3), type II (n = 4), type III (n = 8), and type IV (n = 16) lymphadenopathy. The immunohistochemical and ISH findings are summarized in Table 3. Immunohistochemistry revealed numerous IgG4$^+$ cells ranging from 122 to 477/HPF (mean ± SD, 250 ± 102), and ratios of IgG4$^+$/IgG$^+$ cells were >0.4 in all cases. Greater than 10 EBER$^+$ cells/0.5 cm^2 were found in 18 of 31 cases (58%) with no significant differences in the rates of positivity between the 4 subgroups (2/3 type I, 2/4 type II, 5/8 type III, 9/16 type IV). EBER latency was classified into latency I in examined EBER$^+$ cases (LN12 and LN13). In 15 of 18 cases, scattered EBER$^+$ lymphocytes were seen in interfollicular areas. Two type III cases (cases LN12 and LN13) had numerous diffusely distributed EBER$^+$ cells, with some in intrafollicular areas as well (Fig. 1). EBER$^+$ cells included small lymphocytes and immunoblasts, as is found in AITL.[13] EBER$^+$ cells were localized in germinal centers in 1 type IV case (case LN25); this case also displayed epithelioid granuloma (Fig. 2). All 9 patients with EBER$^+$ type IV IgG4-related lymphadenopathy had systemic lymphadenopathy and/or extranodal involvement. PCR studies for TCR and IGH rearrangements did not demonstrate evidence of clonal T or B cells in 5/5 tested cases (LNs 2, 11, 12, 13, and 14).

Comparison Between EBER$^+$ and EBER$^-$ Cases

There were no differences in age between EBER$^+$ (51 to 76 y; mean ± SD, 64.0 ± 10.2 y) and EBER$^-$ cases (36

TABLE 3. Summary of Clinicopathologic Features of IgG4-related Lymphadenopathy

	Type I (n = 3)	Type II (n = 4)	Type III (n = 8)	Type IV (n = 16)
Age (y)				
Mean ± SD	63.6 ± 8.9	61.5 ± 19	72.5 ± 6.9	61.5 ± 10.8
> 50 y old (n [%])	3 (100)	3 (75)	8 (100)	13 (81)
> 60 y old (n [%])	1 (33)	3 (75)	7 (88)	11 (69)
Sex (Male/Female)	3/0	1/3	6/2	14/2
The number of IgG4$^+$ cells (/HPF)				
Mean ± SD	345 ± 116	155 ± 13.3	337 ± 47.3	198 ± 81.6
IgG4$^+$/IgG$^+$ plasma cell ratio (%)				
Mean ± SD	84.0 ± 14.3	50.2 ± 10.5	73.2 ± 12.7	72.5 ± 15.4
Disease distribution (n [%])				
Localized lymphadenopathy	0 (0)	0 (0)	0 (0)	4 (25)
Systemic lymphadenopathy	3 (100)	4 (100)	8 (100)	2 (13)
With extranodal involvement	1 (33)	3 (75)	3 (38)	12 (75)
EBER-ISH positivity	2 (75)	2 (50)	5 (63)	9 (56)
Distribution (n [%])				
Interfollicular/scattered	2 (100)	2 (100)	3 (60)	8 (88)
Intrafollicular/localized	0 (0)	0 (0)	0 (0)	1 (12)
Diffuse	0 (0)	0 (0)	2 (40)	0 (0)
Age (n [%])				
> 50 y old	2 (100)	1 (50)	5 (100)	8 (88)
> 60 y old	1 (50)	1 (50)	4 (80)	7 (77)

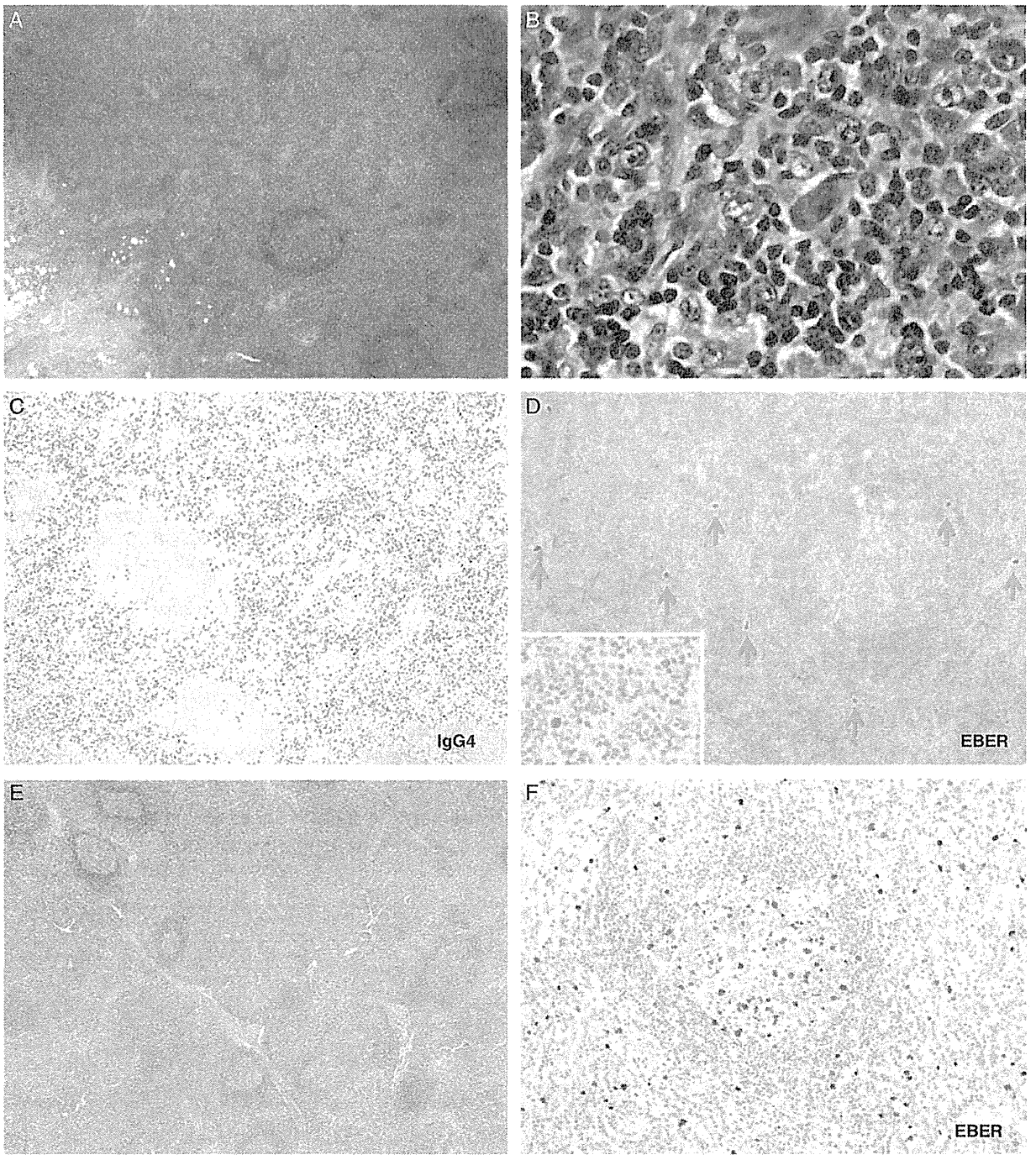

FIGURE 1. Histologic and immunohistochemical studies on type III IgG4-related lymphadenopathy (A–D, LN14; E–F, LN13). A and B, Expanded interfollicular area reveals polymorphous population consisting of mature and immature plasma cells, eosinophils, and numerous immunoblasts with small vessel proliferation (A and B, H&E). C, IgG4$^+$ plasma cells (C, IgG4). D, Small to large EBER-ISH$^+$ cells (133/0.5 cm^2) in the interfollicular area (D, EBER-ISH). E, Expanded interfollicular areas of LN13 (E, H&E). F, Diffuse infiltration of EBER$^+$ cells (F, EBER-ISH). H&E indicates hematoxylin and eosin.

to 82 y; mean ± SD, 65.3 ± 13.8 y) of IgG4-related lymphadenopathy ($P = 0.764$). There was also no difference in serum IgG levels between EBER$^+$ (mean ± SD, 3115 ± 1468 mg/dL; n = 15) and EBER$^-$ (mean ± SD, 2748 ± 1581 mg/dL; n = 12) cases ($P = 0.539$). There was no significant difference in the numbers of FOXP3$^+$ cells

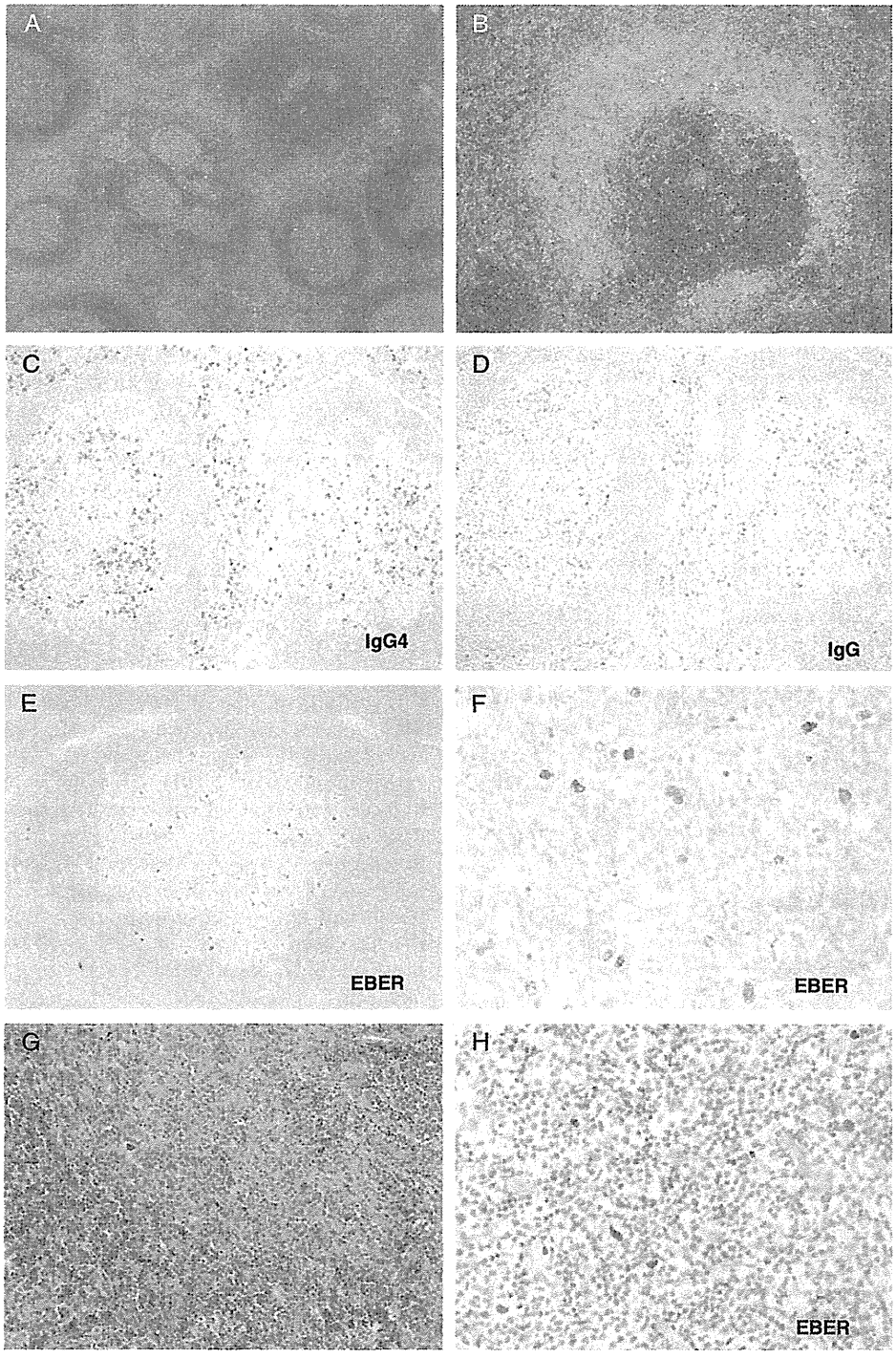

FIGURE 2. Histologic and immunohistochemical features of PTGC-type IgG4-related lymphadenopathy (LN25). A, PTGC-like germinal centers are observed (H&E). B, Epithelioid granuloma (H&E). C and D, Numerous $IgG4^+$ cells are localized in germinal centers. $IgG4^+/IgG^+$ cell ratio is >40% (C, IgG4; D, IgG). E and F, Many EBER-ISH^+ cells localize in a PTGC-like germinal center (E and F, EBER-ISH). G and H, IgG4-related lacrimal gland disease in the same patient (Ex7). G, Fibrosis and lymphoplasmacytic infiltration (H&E). H, Increased $EBER^+$ lymphocytes (56/0.5 cm^2) (EBER-ISH). H&E indicates hematoxylin and eosin.

between EBER$^+$ (mean ± SD, 304 ± 134; n = 11) and EBER$^-$ (mean ± SD, 322 ± 189; n = 8) cases (P = 0.809).

IgG4$^-$ Reactive Lymphoid Hyperplasia

Clinicopathologic and demographic characteristics of IgG4$^-$ reactive lymphoid hyperplasia are listed in Table 4. The age distribution was similar to that of the patients with IgG4-related lymphadenopathy and ranged from 50 to 85 years (mean ± SD, 67.1 ± 12.0). There were 18% of cases (4/22) with > 10 EBER$^+$ cells/0.5 cm^2 (ranging from 35 to 395/0.5 cm^2; mean ± SD, 155 ± 162), a significantly lower proportion than was seen in cases of IgG4-related lymphadenopathy (P = 0.002).

Extranodal IgG4-related Disease

The clinicopathologic findings for cases of extranodal IgG4-related diseases are listed in Tables 5 and 6. Greater than 10 EBER$^+$ cells/0.5 cm^2 were detected in 3 of 9 cases (33%) of IgG4-related lacrimal gland disease, 2 of 10 cases (20%) of IgG4-related submandibular gland disease, 0 of 2 cases (0%) of IgG4-related skin disease, and 0 of 3 cases of IgG4-related pancreatitis (Fig. 3). Although cases Ex4 and Ex7 had EBER$^+$ lymph nodes, only case Ex7 had EBV positivity in the lacrimal gland (Fig. 2G, H). In total, > 10 EBER$^+$ cells/0.5 cm^2 were detected in 5 of 24 (21%) extranodal IgG4-related biopsies, which was significantly less frequent than IgG4-related lymphadenopathy (P = 0.006).

IgG4$^+$ Cells in AITL

Seven cases showed few IgG4$^+$ cells (0 to 5/HPF). Three cases revealed scattered IgG4$^+$ cells (19, 24, and 47/HPF, respectively); none was in the range of the cases with nodal IgG4-related disease. In addition, overall, there were significantly fewer IgG4$^+$ cells present compared with type III IgG4-related lymphadenopathy (mean ± SD, 10.6 ± 15.3 compared with 337 ± 47.3) (P < 0.001).

TABLE 4. Clinicopathologic Features of IgG4$^-$ Reactive Lymphoid Hyperplasia

No.	Age/Sex	Affected Lymph Nodes	EBER-ISH$^+$ Cells (/0.5 cm^2)
RLH1	84/F	Cervix	103
RLH2	69/M	Para-aorta	0
RLH3	79/M	Axilla	0
RLH4	78/F	Inguen	6
RLH5	79/F	Mediastinum	0
RLH6	69/F	Inguen	0
RLH7	63/F	Cervix	0
RLH8	51/F	Inguen	5
RLH9	56/F	Cervix	0
RLH10	50/M	Cervix	395
RLH11	52/M	Cervix	8
RLH12	80/M	Inguen	2
RLH13	78/M	Cervix	1
RLH14	85/F	Axilla	4
RLH15	59/M	Inguen	7
RLH16	72/M	Cervix	0
RLH17	62/M	Inguen	35
RLH18	55/F	Abdomen	0
RLH19	55/F	Axilla	0
RLH20	67/F	Axilla	90
RLH21	53/F	Axilla	4
RLH22	82/M	Cervix	0

F indicates female; M, male; RLH, reactive lymphoid hyperplasia.

DISCUSSION

Very limited previous reports have indicated a possible relationship between IgG4-related disease and EBV. Acute EBV mononucleosis has been reported to be associated with a transient 75% increase in mean serum IgG4 levels.[14] A case of EBV-related lymphadenopathy has been reported that mimicked the clinical features of IgG4-related disease, with an elevated serum IgG4 level but without many IgG4$^+$ cells in the biopsied lymph nodes.[15] EBV$^+$ classical Hodgkin lymphoma was found in a patient with IgG4-related cervical fibrosis.[16] An EBV$^+$ inflammatory pseudotumor-like follicular dendritic cell sarcoma was also reported to have numerous IgG4$^+$ cells.[17] The authors discussed a relationship between EBV-related immune dysfunction and the proliferation of IgG4$^+$ cells. Although these reports mentioned some relationship between EBV and increase of IgG4, EBV infection in IgG4-related disease has not been examined except for a single case report.[5] Hence, this study investigated the relationship between EBV and IgG4-related disease. Increased EBV-infected cells were found in 18 of 31 lymph nodes (58%) with IgG4-related lymphadenopathy. This proportion was significantly higher than that of reactive lymphoid hyperplasia in similarly aged group, which confirmed the clear relationship between IgG4-related lymphadenopathy and EBV. As most Japanese are infected by EBV in childhood, and new onset infection in adulthood is very rare, the increased numbers of EBV$^+$ cells was considered to most likely represent EBV reactivation rather than acute infection.

Type III IgG4-related lymphadenopathy has distinct histologic features, including interfollicular lymphoplasmacytic infiltration, angiogenesis, and many immunoblasts, which mimic AITL.[1] In this study, only a few scattered IgG4$^+$ cells were detected in AITL, which indicated that IgG4$^+$ cell proliferation was not simply induced by EBV reactivation or dysfunction of helper T cells. There is a possibility that both IgG4-related disease and EBV reactivation are induced by other factors.

Type IV cases are usually localized in submandibular lymph nodes, although approximately 50% of cases have extranodal involvement. Less than 10% develop systemic lymphadenopathy.[2] In contrast, in this study, all the patients with type IV IgG4-related lymphadenopathy with EBV reactivation developed systemic lymphadenopathy and/or extranodal involvement. The lymph node in 1 EBV$^+$ type IV case had epithelioid granulomas, which was similar to a previously reported case of EBV$^+$ IgG4-related lymphadenopathy.[5] Cases of IgG4-related lymphadenopathy with epithelioid granulomas have been reported sporadically.[18] Of interest,

TABLE 5. Clinicopathologic Features of Extranodal IgG4-related Diseases

No.	Age/Sex	Affected Organs	Average IgG4$^+$ Cells (/HPF)	EBER-ISH$^+$ Cells (/0.5 cm^2)	Other Lesions
Ex1	56/F	Lacrimal gland	111	1	
Ex2	60/F	Lacrimal gland	282	1	
Ex3	49/M	Lacrimal gland	377	9	
Ex4*	36/F	Lacrimal gland	239	2	Cervical lymph node
Ex5	61/M	Lacrimal gland	373	0	
Ex6	39/F	Lacrimal gland	301	0	
Ex7†	68/M	Lacrimal gland	204	56	Submandibular lymph node
Ex8	67/F	Lacrimal gland	177	175	
Ex9	72/M	Lacrimal gland	231	542	
Ex10	57/F	Submandibular gland	109	0	
Ex11	57/F	Submandibular gland	144	0	Parotid gland
Ex12	59/M	Submandibular gland	190	1	
Ex13	61/M	Submandibular gland	216	5	
Ex14	69/M	Submandibular gland	435	7	
Ex15	76/M	Submandibular gland	160	3	
Ex16	66/F	Submandibular gland	404	2	
Ex17	59/F	Submandibular gland	264	0	
Ex18	69/M	Submandibular gland	307	66	
Ex19	67/M	Submandibular gland	224	157	
Ex20	65/M	Skin	189	0	
Ex21	63/F	Skin	46	0	Parotid gland
Ex22	69/M	Pancreas	195	0	
Ex23	61/M	Pancreas	437	0	
Ex24	64/M	Pancreas	76	0	

*The same patient had IgG4-related lymphadenopathy listed in Table 1 (LN6).
†The same patient had IgG4-related lymphadenopathy listed in Table 1 (LN25).
Ex indicates extranodal; F, female; M, male.

EBER$^+$ cells were localized in germinal centers in this type IV case with epithelioid granuloma. There are reports of EBV$^+$ nonendemic Burkitt lymphoma associated with epithelioid granulomas.[19,20] The significance of this finding is still unclear.

EBV-infected cells are usually observed and studied in the lymph nodes, where the virus is known to remain in the dormant stage for many years.[10] In this study, increased numbers of EBER$^+$ cells were significantly more frequently observed in IgG4-related lymphadenopathy than in extranodal IgG4-related disease. The proportion of EBV$^+$ cases was similar between extranodal IgG4-related disease and non–IgG4-related reactive lymphoid hyperplasia ($P = 0.559$). Increased numbers of EBV-infected cells may be observed more frequently in lymph nodes than in other sites. Lacrimal glands and salivary glands seemed to have increased numbers of EBV-infected cells more frequently than other extranodal sites; however, the number of extranodal samples was too small for a meaningful statistical analysis.

Although our study clearly suggested a relationship between IgG4-related disease and EBV, the precise mechanism remains unclear. Whether IgG4-related disease directly or indirectly induces expansion of EBV-infected cells, possibly related to EBV reactivation, or is secondary to EBV infection is unknown. As mentioned above, acute EBV infection can lead to an increase in the serum IgG4 level. However, in other situations like AITL, EBV-infected cells do not lead to increased numbers of IgG4$^+$ cells, suggesting that IgG4 lymphadenopathy is not the direct effect of EBV infection and that the increased number of EBV$^+$ cells, present in only a subset of cases, is somehow related to the IgG4 disease.

Because of concern as to whether the expansion of EBV-infected cells in many cases of IgG4-related lymphadenopathy could simply reflect an age-related phenomenon, a group of non–IgG4-related reactive lymph nodes were studied for comparison purposes. This patient cohort did not show a difference in age from the patients with IgG4-related disease but had significantly fewer cases with increased EBV-infected cells. In addition, there was no significant difference in age distribution between EBER$^+$ and EBER$^-$ IgG4-related disease cases. Therefore, age does not seem to be a factor in the association of IgG4-related nodal disease with increased numbers of EBV-infected cells.

Upregulation of Treg and helper T-cell (Th2) activity has been reported in tissues with IgG4-related

TABLE 6. Summary of Clinicopathologic Features of IgG4-related Diseases

	Lymph Node (n = 31)	Lacrimal Gland (n = 9)	Submandibular Gland (n = 10)	Skin (n = 2)	Pancreas (n = 3)
Age (y)	64.5 ± 11.6	56.4 ± 12.7	64.0 ± 6.0	64.0 ± 1.4	64.6 ± 4.0
Sex	M:F = 24:7	M:F = 4:5	M:F = 6:4	M:F = 1:1	M:F = 3:0
EBER$^+$ cases (n [%])	18 (58)	3 (33)	2 (20)	0 (0)	0 (0)

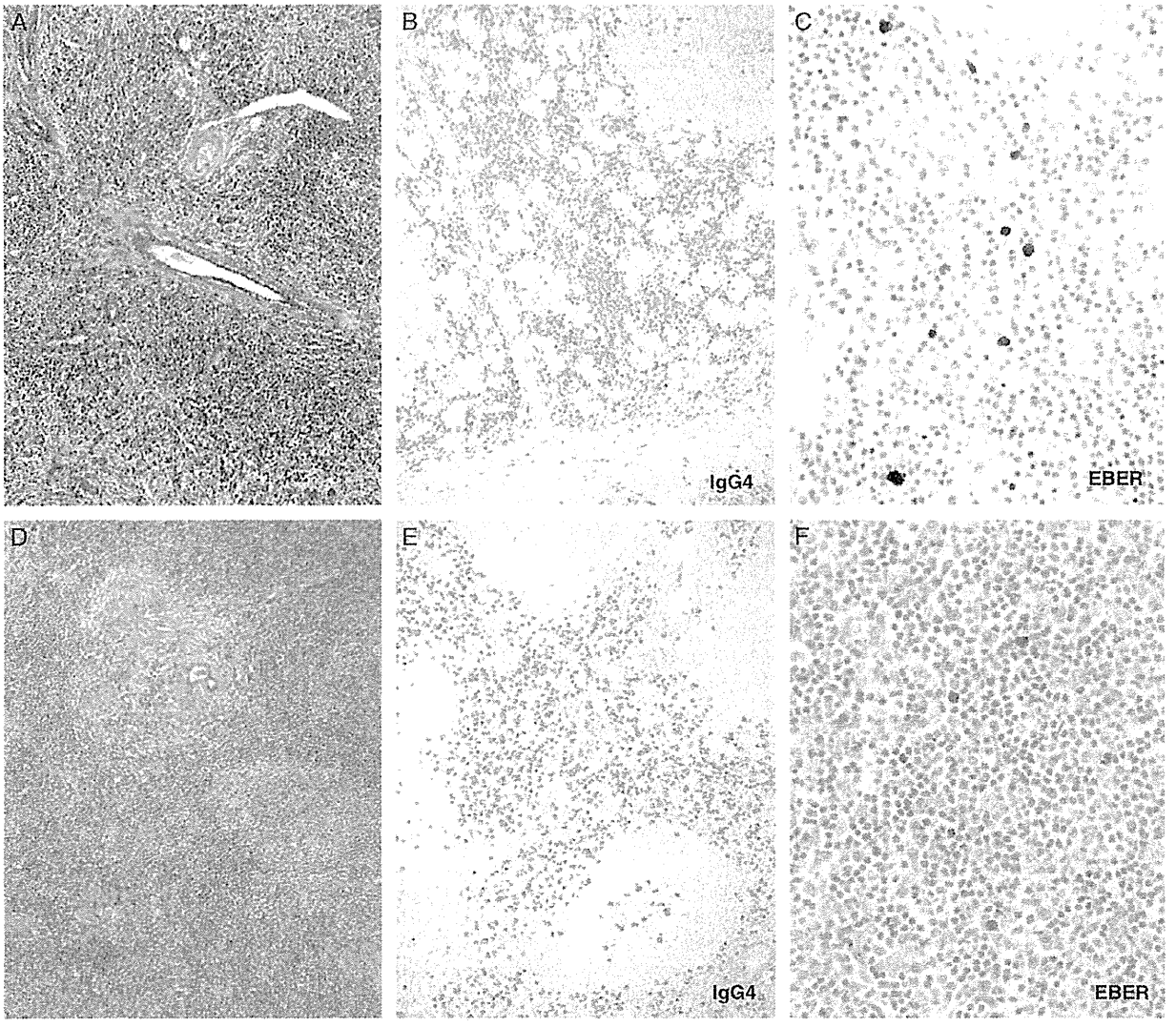

FIGURE 3. Analysis of extranodal IgG4-related disease: IgG4-related submandibular gland disease (Ex19). A, Lymphoplasmacytic infiltration and dense fibrosis. Salivary gland ducts remain intact (H&E). B, Numerous IgG4$^+$ cells (IgG4). C, Increased EBER$^+$ cells (157/0.5 cm^2) (EBER-ISH). D–F, IgG4-related lacrimal gland disease (Ex9). D, Infiltration of small lymphocytes and plasma cells (H&E). E, Significant IgG4$^+$ cells (IgG4). F, Increased EBER$^+$ cells (542/0.5 cm^2) (EBER-ISH). H&E indicates hematoxylin and eosin.

disease.[3] Although the precise mechanism of immune suppression by Treg is not fully understood, secretion of interleukin-10 and transforming growth factor β1 seems to be involved.[21] Although the relationship between Treg and EBV has not been fully investigated, upregulation of Treg activity might contribute to a disruption of immune balance. However, in our study, the number of FOXP3$^+$ Tregs was similar between EBER$^+$ and EBER$^-$ groups. Further study is required to understand the relationship between IgG4-related disease and EBV.

In conclusion, increased numbers of EBV-infected cells are frequently found in IgG4-related lymphadenopathy, including in the type III cases with many immunoblasts that can morphologically mimic AITL, and is not related to patient age. Distinction from AITL, however, was not difficult, in part because AITL never had sufficient IgG4 positivity to fulfill the criteria for IgG4-related lymphadenopathy. IgG4-related disease with increased numbers of EBER$^+$ cells may have some clinical implications as, in contrast to usual expectation, all the patients with EBV$^+$ type IV IgG4-related lymphadenopathy developed systemic lymphadenopathy and/or extranodal involvement. Finally, particularly given that IgG4-related lymphadenopathy often occurs in individuals over 50 years of age, it is important to recognize that it must be included in the differential diagnosis of EBV$^+$ lymphoproliferative disorders, including EBV$^+$ diffuse large B-cell lymphoma of the elderly.

ACKNOWLEDGMENTS

This work was supported by a Grant-in-Aid for Scientific Research (C) (no. 24591447) from the Japan Society for the Promotion of Science and 'Research on Measures for Intractable Disease' Project: matching fund subsidy from Ministry of Health Labour and Welfare, Japan.

REFERENCES

1. Sato Y, Notohara K, Kojima M, et al. IgG4-related disease: histological overview and pathology of hematological disorders. *Pathol Int.* 2010;60:247–258.
2. Sato Y, Inoue D, Asano N, et al. Association between IgG4-related disease and progressively transformed germinal centers of lymph nodes. *Mod Pathol.* 2012;35:956–967.
3. Zen Y, Fujii T, Harada K, et al. Th2 and regulatory immune reactions are increased in immunoglobin G4-related sclerosing pancreatitis and cholangitis. *Hepatology.* 2007;45:1538–1546.
4. Niedobitek G, Herbst H, Young LS, et al. Patterns of Epstein-Barr virus infection in non-neoplastic lymphoid tissue. *Blood.* 1992; 79:2520–2526.
5. Takahashi E, Kojima M, Kobayashi M, et al. Primary IgG4-related lymphadenopathy with prominent granulomatous inflammation and reactivation of Epstein-Barr virus. *Virchows Arch.* 2012;460: 225–229.
6. Deshpande V, Zen Y, Chan JK, et al. Consensus statement on the pathology of IgG4-related disease. *Mod Pathol.* 2012;25: 1181–1192.
7. Sato Y, Kojima M, Takata K, et al. Systemic IgG4-related lymphadenopathy: a clinical and pathologic comparison to multicentric Castleman's disease. *Mod Pathol.* 2009;22:589–599.
8. Sato Y, Takeuchi M, Takata K, et al. Clinicopathologic analysis of IgG4-related skin disease. *Mod Pathol.* 2013;26:523–532.
9. Dogan A, Gaulard P, Jaffe ES, et al. Angioimmunoblastic T-cell lymphoma. In: Swerdlow SH, Campo E, Harris NL, eds. *WHO Classification of Tumours of Haematopoietic and Lymphoid Tissues.* Lyon, France: International Agency for Research on Cancer; 2008: 309–311.
10. Dojcinov SD, Venkataraman G, Pittaluga S, et al. Age-related EBV-associated lymphoproliferative disorders in the Western population: a spectrum of lymphoid hyperplasia and lymphoma. *Blood.* 2011;117:4726–4735.
11. van Dongen JJ, Langerak AW, Bruggemann M, et al. Design and standardization of PCR primers and protocols for detection of clonal immunoglobulin and T-cell receptor gene recombinations in suspect lymphoproliferations: report of the BIOMED-2 Concerted Action BMH4-CT98-3936. *Leukemia.* 2003;17:2257–2317.
12. Miyata-Takata T, Takata K, Yamanouchi S, et al. Detection of T-cell receptor γ gene rearrangement in paraffin-embedded T or natural killer/T-cell lymphoma samples using the BIOMED-2 protocol. *Leuk Lymphoma.* 2014. [Epub ahead of print].
13. Federico M, Rudiger T, Bellei M, et al. Clinicopathologic characteristics of angioimmunoblastic T-cell lymphoma: analysis of the international peripheral T-cell lymphoma project. *J Clin Oncol.* 2013;31:240–246.
14. Shacks SJ, Heiner DC, Bahba SL, et al. Increased serum IgG4 levels in acute Epstein-Barr viral mononucleosis. *Ann Allergy.* 1985;54:284–288.
15. Wada Y, Kojima M, Yoshita K, et al. A case of Epstein-Barr virus-related lymphadenopathy mimicking the clinical features of IgG4-related disease. *Mod Rheumatol.* 2013;23:597–603.
16. Cheuk W, Tam F, Chan A, et al. Idiopathic cervical fibrosis-A new member of IgG4-related sclerosing diseases: report of 4 cases, 1 complicated by composit lymphoma. *Am J Surg Pathol.* 2010; 34:1678–1685.
17. Choe JY, Go H, Jeon YK, et al. Inflammatory pseudotumor-like follicular dendritic cell sarcoma of the spleen: a report pf six cases with increased IgG4+ cells. *Pathol Int.* 2013;63:245–251.
18. Zen Y, Nakamura Y. IgG4-related disease: a cross-sectional study of 114 cases. *Am J Surg Pathol.* 2010;34:1812–1819.
19. Haralambieva E, Rosati S, Noesel CN, et al. Florid granulomatous reaction in Epstein-Barr virus-positive nonendemic Burkitt lymphomas. *Am J Surg Pathol.* 2004;28:379–383.
20. Schrager JA, Pittaluga S, Raffeld M, et al. Granulomatous reaction in Burkitt lymphoma: correlation with EBV positivity and clinical outcome. *Am J Surg Pathol.* 2005;29:1115–1116.
21. Wingate PJ, McAulay KA, Anthony IC, et al. Regulatory T cell activity in primary and persistent Epstein-Barr virus infection. *J Med Virol.* 2009;81:870–877.

和田　聡
(神奈川県立がんセンター)

Cancer Science
Japanese Cancer Association JCA Open Access

Stathmin1 regulates p27 expression, proliferation and drug resistance, resulting in poor clinical prognosis in cholangiocarcinoma

Akira Watanabe,[1] Hideki Suzuki,[1] Takehiko Yokobori,[1] Mariko Tsukagoshi,[1] Bolag Altan,[1] Norio Kubo,[1] Shigemasa Suzuki,[1] Kenichiro Araki,[1] Satoshi Wada,[1] Kenji Kashiwabara,[2] Yasuo Hosouchi[3] and Hiroyuki Kuwano[1]

[1]Department of General Surgical Science, Gunma University Graduate School of Medicine, Gunma; [2]Pathological Department, Gunma Prefecture Saiseikai-Maebashi Hospital, Gunma; [3]Department of Surgery and Laparoscopic Surgery, Gunma Prefecture Saiseikai-Maebashi Hospital, Gunma, Japan

Key words
Cancer progression, drug resistance, extrahepatic cholangiocarcinoma, p27, stathmin1

Correspondence
Akira Watanabe, Department of General Surgical Science (Surgery I), Gunma University Graduate School of Medicine, 3-39-22 Showa-machi, Maebashi, Gunma 371-8511, Japan.
Tel: +81 2 7220 8224; Fax: +81 2 7220 8230;
E-mail: akira_watanabe@gunma-u.ac.jp

Funding information
None declared.

Received February 9, 2014; Revised April 3, 2014; Accepted April 6, 2014

*Cancer Sci*105 (2014) 690–696

doi: 10.1111/cas.12417

Patients with extrahepatic cholangiocarcinoma (EHCC) have a poor prognosis; postoperative survival depends on cancer progression and therapeutic resistance. The mechanism of EHCC progression needs to be clarified to identify ways to improve disease prognosis. Stathmin1 (STMN1) is a major cytosolic phosphoprotein that regulates microtubule dynamics and is associated with malignant phenotypes and chemoresistance in various cancers. Recently, STMN1 was reported to interact with p27, an inhibitor of cyclin-dependent kinase complexes. Eighty EHCC cases were studied using immunohistochemistry and clinical pathology to determine the correlation between STMN1 and p27 expression; RNA interference to analyze the function of STMN1 in an EHCC cell line was also used. Cytoplasmic STMN1 expression correlated with venous invasion ($P = 0.0021$) and nuclear p27 underexpression ($P = 0.0011$). Patients in the high-STMN1-expression group were associated with shorter recurrence-free survival and overall survival than those in the low-expression group. An *in vitro* protein-binding assay revealed that cytoplasmic STMN1 bound to p27 in the cytoplasm, but not in the nucleus of EHCC cells. Moreover, p27 accumulated in EHCC cells after STMN1 suppression. STMN1 knockdown inhibited proliferation and increased the sensitivity of EHCC cells to paclitaxel. STMN1 contributes to a poor prognosis and cancer progression in EHCC patients. Understanding the regulation of p27 by STMN1 could provide new insights for overcoming therapeutic resistance in EHCC.

Cholangiocarcinoma is associated with poor prognosis and its incidence and mortality are increasing worldwide.[1] The 5-year survival rate for cholangiocarcinoma is 10–40%.[2] Cholangiocarcinoma is defined as intrahepatic or extrahepatic (EHCC), the latter of which consists of hilar or bile duct tumors. Surgical therapy is the only effective curative treatment for EHCC; postoperative survival is dependent on the existence of invasion and metastasis.[3,4] Therefore, to improve patient prognoses, we must understand the mechanism of cancer progression in EHCC.

Stathmin1 (STMN1) is a major cytosolic phosphoprotein that regulates microtubule dynamics by preventing tubulin polymerization and promoting microtubule destabilization. STMN1 plays an important role in a variety of biological processes, including carcinogenesis. STMN1 is highly expressed in various types of human malignancies and is therefore also known as oncoprotein 18 (OP18). Moreover, STMN1 expression correlates with tumor progression and poor prognosis in the following cancers: breast cancer,[5–7] prostate cancer,[8] gastric cancer,[9,10] hepatocellular carcinoma,[11,12] oral squamous cell carcinoma,[13] colorectal cancer,[14,15] malignant mesothelioma[16] and urothelial carcinoma.[17] Thus, *STMN1* is a fundamental cancer-associated gene and a potential target for diagnosis and treatment. To our knowledge, STMN1 expression in EHCC has not been reported; therefore, we explored the role of STMN1 in EHCC.

STMN1 regulates microtubule metabolism and contributes to tumor progression. Baldassarre *et al.*[18] reported that STMN1 bound to p27 suppressed the function of p27 and enhanced the proliferation of tumor cells. p27 was discovered as an inhibitor of cyclin-dependent kinase (CDK) complexes in TGF (transforming growth factor) β-arrested cells and was classified as a member of the Cip/Kip family of cyclin-dependent kinase inhibitors (CKI).[19] The CKI associate with a broad spectrum of cyclin–CDK complexes to negatively regulate progression through the G1 phase of the cell cycle. More recently, cytoplasmic p27 was shown to play a role in the regulation of cell migration.[20] However, there are still few reports that discuss the relationship of STMN1 and p27 in malignancy, including EHCC. Therefore, we examined the relationship between STMN1 and p27 in EHCC.

The purpose of the present study was to clarify the function of STMN1 in EHCC cell lines *in vitro*, determine the clinical significance of STMN1 in primary EHCC and evaluate the relationship between STMN1 and p27. To this end, we performed immunohistochemistry to evaluate the relationships between STMN1, p27 and clinicopathological factors in clinical EHCC samples. We also examined the *in vitro* effects of

siRNA-mediated STMN1 suppression on the proliferation, chemotherapeutic sensitivity and p27 expression in human EHCC cell lines.

Material and Methods

Patients and samples. Imunohistochemistry was performed on 80 EHCC patients who had undergone curative surgery in our department between 1995 and 2011. Patients ranged in age from 43 to 94 years. Tumor stage was classified according to the seventh tumor–node–metastasis (TNM) classification of the Union for International Cancer Control (UICC).[21] Forty-four (53%) patients received adjuvant therapy following chemotherapy: 11 received UFT (tegafur-uracil; Taiho Pharmaceutical, Tokyo, Japan); nine received Gemcitabine (Eli Lilly and Company, Indianapolis, IN, USA); 21 received S-1 (TS-1; Taiho Pharmaceutical); and three received Gemcitabine+S-1. All patients provided written informed consent, as per institutional guidelines.

Immunohistochemical staining. A 4-μm section was cut from paraffin blocks of EHCC samples. Each section was mounted on a silane-coated glass slide, deparaffinized and soaked for 30 min at room temperature in 0.3% H_2O_2/methanol to block endogenous peroxidases. The sections were then heated in boiled water and Immunosaver (Nishin EM, Tokyo, Japan) at 98°C for 45 min. Non-specific binding sites were blocked by incubating with Protein Block Serum-Free (DAKO, Carpinteria, CA, USA) for 30 min. A mouse monoclonal anti-STMN1 (OP18) antibody (Santa Cruz Biotechnology, Santa Cruz, CA, USA) and a mouse monoclonal anti-p27 antibody (Santa Cruz Biotechnology) were applied at a dilution of 1:100 for 24 h at 4°C. The primary antibody was visualized using the Histofine Simple Stain PO (M) Kit (Nichirei, Tokyo, Japan) according to the instruction manual. The chromogen 3,3¢-diaminobenzidine tetrahydrochloride was applied as a 0.02% solution containing 0.005% H_2O_2 in 50 mM ammonium acetate-citrate acid buffer (pH 6.0). The sections were lightly counterstained with Mayer's hematoxylin and mounted. Negative controls were established by omitting the primary antibody and no detectable staining was evident. We previously confirmed that esophageal carcinomas express STMN1 and p27; therefore, esophageal carcinomas were used as a positive control (Figs S1–S3).

Immunohistostaining results were evaluated as described by Altan *et al.*[22] The intensity of cytoplasmic STMN1, nuclear p27 and cytoplasmic p27 staining was scored as follows: 0, no staining; 1+, weak staining; 2+, moderate staining; and 3+, strong staining relative to the positive control (Figs S1–S3). The percentage of nuclear-stained cells was calculated by examining at least 1000 cancer cells in five representative areas. Cytoplasmic STMN1, nuclear p27 and cytoplasmic p27 were scored as follows: 0, no staining; 1+, 1–10%; 2+, 11–50%; and 3+, 51–100%. The score was defined as the percentage score multiplied by the intensity score according to the criteria presented in Table S1 (0, 1+, 2+, 3+, 4+, 6+ and 9+). The optimal cut-off point was defined as follows: grades 0, 1, 2, 3 and 4 were considered low expression, while grades 6 and 9 were designated as high expression. All samples were evaluated by two observers (AW, TY). The Ki-67 labeling index was used to calculate the percentage of cells with high nuclear expression cells in approximately 1000 cells per sample.[23]

Cell culture. The human EHCC cell line HuCCT-1 was used in the present study. All cells were obtained from RIKEN BRC through the National Bio-Resource Project of MEXT, Tokyo, Japan. The cells were cultured in RPMI 1640 medium (Wako, Osaka, Japan) supplemented with 10% FBS and 1% penicillin–streptomycin (Invitrogen, Carlsbad, CA, USA).

siRNA transfection. STMN1-specific siRNA (Silencer Pre-designed siRNA) was purchased from Bonac Corporation (Fukuoka, Japan). HuCCT-1 cells were seeded in six-well, flat-bottom microtiter plates at a density of 1×10^5 cells per well in a volume of 2 mL and incubated in a humidified atmosphere (37°C and 5% CO_2). After incubation, 500 μL of Opti-MEM I Reduced Serum Medium (Invitrogen), 5 μL Lipofectamine RNAi MAX (Invitrogen) and 5 μL STMN1-specific siRNA (50 nM final concentration in each well) were mixed and incubated for 20 min to form chelate bonds. The siRNA reagents were then added to the cells. The experiments were performed after 24–96 h of incubation.

Proximity ligation assay (PLA). HuCCT1 cells were seeded and incubated on Chamber Slides (Lab-Tek II, Thermo Scientific, Waltham, MA, USA) for 24 h. The cells were fixed with 4% paraformaldehyde for 30 min and 100% methanol for 10 min. The slides were then blocked in 4% bovine serum albumin (Millipore, Biillerica, MA, USA) for 30 min and incubated for 48 h at 4°C with the appropriate combinations of mouse, rabbit and goat antibodies diluted 1:100 (STMN1 rabbit antibody; Cell Signaling Technology, Danvers, MA, USA; and p27 mouse antibody; Santa Cruz Biotechnology) in antibody dilution solution (Olink Bioscience, Uppsala, Sweden). After washing, the slides were incubated with Duolink PLA Rabbit MINUS and PLA Mouse PLUS proximity probes (Olink Bioscience) and a proximity ligation was performed using the Duolink Detection Reagent Kit (Olink Bioscience) according to the manufacturer's protocol. Nuclei were stained with Duolink In Situ Mounting Medium with DAPI (Olink Bioscience). Images were acquired with an All-in-one Fluorescence Microscope (Keyence Corporation, Osaka, Japan).

Protein extraction and western blot analysis. Transfected cells were incubated for 96 h. Total protein was extracted using the PRO-PREP Protein Extraction Solution Kit (iNtRON Biotechnology, Sungnam, Kyungki-Do, Korea) and nuclear protein was extracted with the NE-PER Nuclear and Cytoplasmic Extraction Kit (Thermo Scientific, Kanagawa, Japan). The proteins were separated on 4–12% Bis-Tris Mini Gels (Life Technologies Corporation, Carlsbad, CA, USA) and transferred to membranes using an iBlot Dry Blotting System (Life Technologies Corporation). The membranes were incubated overnight at 4°C with mouse monoclonal antibodies against STMN1 (1:1000; Santa Cruz Biotechnology), p27 (1:1000; Santa Cruz Biotechnology), β-actin (1:1000; Sigma, St Louis, MO, USA) and Histone H1 (1:1000; Santa Cruz Biotechnology). The membranes were then treated with horseradish peroxidase-conjugated anti-mouse secondary antibodies and the proteins were detected with the ECL Prime Western Blotting Detection System (GE Healthcare, Tokyo, Japan).

Proliferation assay. Cell proliferation was measured with the Cell Counting Kit-8 (Dojindo Laboratories, Kumamoto, Japan). At 48 h after transfection, the HuCCT1 cells were plated (approximately 5000 cells per well) in 96-well plates in 100 μL of medium containing 10% FBS. Evaluations were performed at the following time points: 0, 24, 48, 72 and 96 h. To determine cell viability, 10 μL of cell counting solution was added to each well and incubated at 37°C for 2 h. Next, the absorbance of each well was detected at 450 nm using a xMark Microplate Absorbance Spectrophotometer (Bio Rad, Hercules, CA, USA).

Paclitaxel assay. A water-soluble tetrazolium (WST)-8 test and the Cell Counting Kit-8 (Dojindo Laboratories) were used to evaluate paclitaxel sensitivity. At 48 h after transfection, HuCCT1 cells were seeded (10 000 cells/well) into 96-well

plates in 100 μL medium containing 10% FBS prior to drug exposure. After 24 h pre-incubation the cells were treated with various concentrations of paclitaxel for 48 h. Then, 10 μL WST-8 reagent was added and the cells were incubated for an additional 2 h at 37°C. Viability was determined using colorimetry by absorbance at 450 nm (xMark Microplate Absorbance Spectrophotometer).

Statistical analysis. Data for the continuous variables are expressed as the mean ± SEM. Significance was determined using Student's *t*-tests and ANOVA. Statistical analysis of the immunohistochemical staining data was performed using the chi-squared test. Survival curves were calculated using the Kaplan–Meier method and analyzed with the log-rank test. Prognostic factors were examined by univariate and multivariate analyses using a Cox proportional hazards model. All differences were deemed significant at $P < 0.05$ and all statistical analyses were performed with JMP software, version 5.01 (SAS Institute Inc., Cary, NC, USA).

Results

Immunohistochemical staining of STMN1 and p27 in EHCC tissues. STMN1 expression was evaluated using immunohistochemistry in 80 EHCC samples. Thirty-three samples (41.2%) were negative for STMN1 expression (Fig. 1a) and 47 samples (58.8%) were positive for cytoplasmic STMN1 expression (Fig. 1b). Nuclear p27 expression was also evaluated in these samples. Twenty-five (31.2%) samples were positive for p27 expression (Fig. 1c) and 55 samples (68.8%) were negative (Fig. 1d). High STMN1 expression was associated with low p27 nuclear expression ($P = 0.0011$; Table 1). Cytoplasmic p27 expression was evaluated in the same EHCC samples; 43 (54.4%) samples demonstrated high cytoplasmic staining for p27 expression (Fig. 1d), whereas 36 (45.6%) samples exhibited low p27 expression (Fig. 1c). High STMN1 expression was associated with high p27 cytoplasmic expression ($P = 0.0063$; Table 1).

STMN1 expression correlates with venous invasion and Ki-67 labeling index in EHCC tissues. The correlations between STMN1 expression and clinicopathological findings are shown in Table 1. We considered the following factors: patient age, patient gender, tumor stage, lymph node metastasis, lymphatic invasion, venous invasion, nerve invasion, infiltrating type and TNM stage (UICC 7th).[21] The results showed a correlation between high STMN1 expression and venous invasion ($P = 0.0021$). We also examined the association between STMN1 expression and the Ki-67 labeling index to evaluate proliferation. High-STMN1-expressing patients had a significantly higher Ki-67 labeling index in comparison to low-STMN1-expressing patients ($P < 0.0001$).

Prognostic significance of STMN1 expression in EHCC. The prognostic significance of STMN1 expression on postoperative recurrence-free survival (RFS) and cancer-specific survival (CSS) is shown in Figure 2. The STMN1-positive group had significantly poorer prognoses than the STMN1-negative group, regarding both RFS ($P = 0.0222$) and CSS ($P = 0.0061$). For CSS, STMN1 expression was prognostic for poor survival in the univariate analysis (Table 2; $P = 0.0044$). Multivariate analysis also showed STMN1 expression is prognostic for poor survival (Table 2; $P = 0.0165$). Interestingly, other existing clinicopathological factors were not significantly and independently associated with shorter CSS, whereas STMN1 expression in EHCC remained more significant than the presence of lymph node metastasis (Table 2; hazard ratio [HR], 1.696; 95% confidence interval [CI], 1.10–2.76).

STMN1 and p27 cross-interact in cultured EHCC cells. To examine the protein complexes of STMN1 and p27 in HuCCT1 cells, we performed PLA, which revealed the complexes as red spots in the cytoplasm (Fig. 3a). Thus, STMN1 interacts with p27 in the cytoplasm, but not in the nucleus, of EHCC cells.

siRNA-mediated STMN1 suppression and p27 expression in HuCCT-1 cells. Two siRNA complexes were used to knock down STMN1 expression in HuCCT-1 cells. Suppression of STMN1 by siRNA1 and siRNA2 was demonstrated using western blotting 96 h after transfection (Fig. 3b). Next, we examined the effect of STMN1 knockdown on p27 expression. STMN1 depletion induced total p27 protein expression and

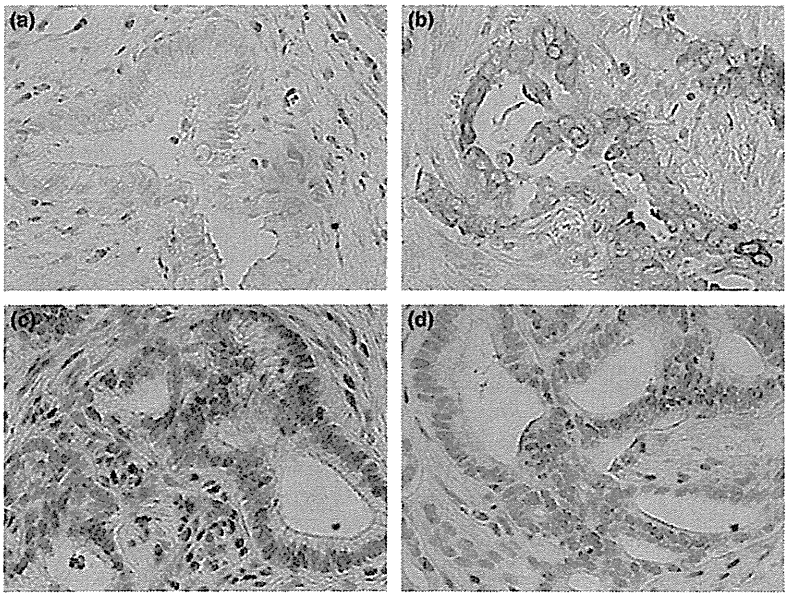

Fig. 1. Immunohistochemical staining of stathmin1 (STMN1) and p27 in primary extrahepatic cholangiocarcinoma (EHCC) samples. (a) Low STMN1 expression in a primary EHCC specimen (original magnification, ×400). (b) High STMN1 expression in a primary EHCC specimen (original magnification, ×400). (c) High nuclear p27 expression and low cytoplasmic p27 expression in a primary EHCC specimen (original magnification, ×400). (d) Low nuclear p27 expression and high cytoplasmic p27 expression in a primary EHCC specimen (original magnification, ×400). Figures a, c and b, d show images from the same cases.

Table 1. Clinicopathological characteristics of extrahepatic cholangiocarcinoma patients according to stathmin expression

Factor	STMN1 low expression (n = 33)	STMN1 high expression (n = 47)	P-value
Age (years)			
≤65	13	18	0.9211
>65	20	29	
Sex			
Male	23	35	0.6389
Female	10	12	
Differentiation			
Well	9	9	0.2563
Moderate	15	26	
Poor	8	14	
Tumor stage			
T1–2	20	19	0.0745
T3–4	13	28	
Lymph node metastasis			
–	19	27	0.9908
+	14	20	
Lymphatic invasion			
–	7	4	0.1070
+	26	43	
Venous invasion			
–	12	4	0.002*
+	21	43	
Distant metastasis			
–	32	45	0.7740
+	1	2	
Infiltration			
α	0	2	0.1179
β	17	31	
γ	15	14	
TNM stage (UICC)			
0, I	11	11	0.3297
II, III, IV	22	36	
Nuclear p27			
High expression	17	8	0.001*
Low expression	16	39	
Cytoplasmic p27			
High expression	12	31	0.006*
Low expression	21	15	
Ki-67 labeling index (mean ± SD)	9.28 ± 13.5	62.1 ± 31.9	<0.0001*

*P < 0.05. STMN1, stathmin1; TNM, tumor–node–metastasis; UICC, Union for International Cancer Control.

also had a tendency to increase nuclear p27 expression (Fig. 3b).

Suppression of STMN1 reduces proliferation and sensitizes EHCC cells to paclitaxel. We assessed the relationship between EHCC proliferation and STMN1 expression. WST assays revealed that the proliferation of STMN1-knockdown cells was significantly lower than in the parent and negative-control cells (P < 0.01; Fig. 3c). STMN1-knockdown cells were also significantly more sensitive to paclitaxel than the control cells (P < 0.01; Fig. 3d).

Immunohistochemical staining of STMN1 and p27 in EHCC tissues. STMN1 expression was evaluated using immunohistochemistry in 80 EHCC samples. Overall, 33 (41.2%) EHCC samples were negative for STMN1 expression (Fig. 1a), whereas 47 (58.8%) samples exhibited positive cytoplasmic staining for STMN1 expression (Fig. 1b). Nuclear p27 expression was also evaluated in the 80 EHCC samples. Twenty-five (31.2%) samples demonstrated positive nucleic staining for p27 expression (Fig. 1c), whereas 55 (68.8%) samples were negative for p27 expression (Fig. 1d). Moreover, the samples exhibiting high STMN1 expression were associated with low p27 nuclear expression (P = 0.0011; Table 1). In addition, p27 expression was also evaluated on each EHCC samples, 43 (54.4%) samples demonstrated high cytoplasmic staining for p27 expression (Fig. 1d), whereas 36 (45.6%) samples were low staining for p27 expression (Fig. 1c). The samples exhibiting high STMN1 expression were also associated with high p27 cytoplasmic expression (P = 0.0063; Table 1).

STMN1 expression correlates with venous invasion and Ki-67 labeling index in EHCC tissues. The correlations between STMN1 expression and clinicopathological findings are displayed in Table 1. Regarding the clinicopathological findings, we considered the following factors: patient age, patient gender, tumor stage, lymph node metastasis, lymphatic invasion, venous invasion, nerve invasion, infiltrating type and TNM stage (UICC 7th). The results revealed that STMN1-high expression was correlated with venous invasion (P = 0.0021). In addition, we examined the association between STMN1 expression and the Ki-67 labeling index to evaluate proliferation ability. The STMN1-high-expression patients had a significantly higher Ki-67 labeling index than the low-expression patients (P < 0.0001).

Prognostic significance of STMN1 expression in EHCC. The prognostic significance of STMN1 expression on postoperative RFS and CSS rates are displayed in Figure 2. The STMN1-positive group had significantly poorer prognoses than the STMN1-negative group, regarding both RFS (P = 0.0222) and CSS (P = 0.0061). For CSS, STMN1 expression was a prognostic factor for poor survival in the univariate analysis (Table 2; P = 0.0044). In the multivariate analysis, STMN1 expression was also a prognostic factor for poor survival (Table 2; P = 0.0165). Interestingly, other existing clinicopathological factors were not significantly and independently associated with shorter CSS, whereas the detection of STMN1 expression in EHCC remained prognostically more significant than the presence of lymph node metastasis with regard to CSS (Table 2; HR, 1.696; 95% CI, 1.10–2.76).

STMN1 and p27 cross-interactinn EHCC cells *in vitro*. To examine the protein complexes formed between STMN1 and p27 in HuCCT1 cells, we performed PLA. As a result, the formations of STMN1 and p27 complexes were detected in the cytoplasm as red spots (Fig. 3a). This result demonstrates that STMN1 interacts with p27 in the cytoplasm, but not in the nucleus, of EHCC cells.

Effect of siRNA-mediated STMN1 suppression on p27 expression in HuCCT-1 cells. Two siRNA complexes were used to knockdown *STMN1* expression in the HuCCT-1 cells. The suppression of STMN1 by siRNA1 and siRNA2 was demonstrated using western blotting 96 h after transfection (Fig. 3b). Next, we examined the effect of *STMN1* knockdown on p27 expression. The depletion of STMN1 increased p27 expression on total protein and also had a tendency to increase nuclear p27 expression (Fig. 3b).

Suppression of STMN1 reduces proliferation and sensitizes EHCC cells to paclitaxel. We assessed the relationship between the proliferative ability of EHCC cells and STMN1 expression. The cellular proliferation ability was evaluated using the WST assay, which revealed that the proliferation of *STMN1*-knockdown cells significantly diminished compared with the

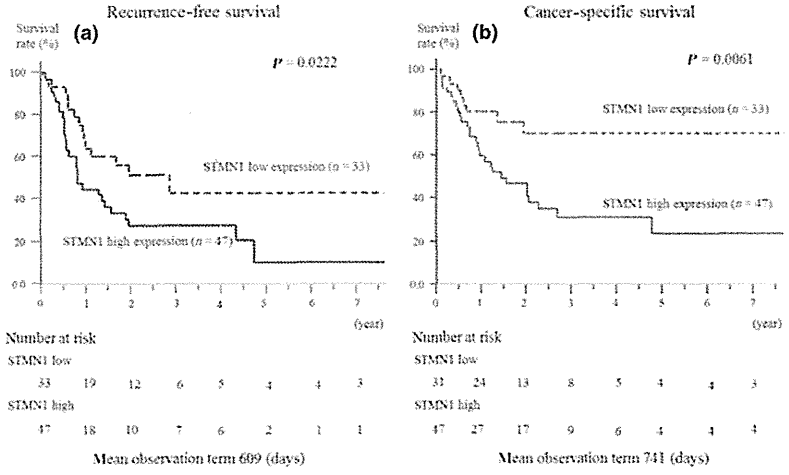

Fig. 2. Relationship between postoperative survival and stathmin1 (STMN1) expression. Kaplan–Meier curves of the low-STMN1-expression and high-STMN1-expression groups are shown. (a) High STMN1 expression indicated a poor prognosis for recurrence-free survival ($P = 0.0222$). (b) High STMN1 expression also indicated a poor prognosis for cancer-specific survival ($P = 0.0061$).

Table 2. Univariate and multivariate analysis of prognostic factors using the Cox proportional hazards model

Factor	Univariate analysis			Multivariate analysis		
	RR	95% CI	*P*-value	RR	95% CI	*P*-value
Age (≤65/>66)	0.994	0.70–1.38	0.9720	–	–	–
Sex (M/F)	0.753	0.49–1.09	0.1392	–	–	–
Tumor stage (T1–2/3–4)	2.314	1.18–4.71	0.0131*	2.031	0.97–4.39	0.0577
Lymph node metastasis (−/+)	1.742	1.23–2.50	0.0013*	1.48	1.02–2.20	0.0379*
Lymphatic invasion (−/+)	1.631	0.97–3.33	0.0649	–	–	–
Venous invasion (−/+)	1.619	1.02–2.97	0.0410*	1.039	0.59–1.99	0.898
Distant metastasis (−/+)	1.803	0.29–5.99	0.4582	–	–	–
Adjuvant therapy (−/+)	0.467	0.25–0.90	0.0242*	0.346	0.17–0.70	0.0035*
Nuclear p27 expression (−/+)	0.596	0.36–0.89	0.0011*	0.811	0.47–1.30	0.401
STMN1 expression (−/+)	1.688	1.16–2.58	0.0044*	1.696	1.10–2.76	0.0165*

*$P < 0.05$. CI, confidence interval; RR, relative risk; STMN1, stathmin1.

parent and negative-control cells ($P < 0.01$; Fig. 3c). Moreover, *STMN1*-knockdown cells exhibited significantly higher sensitivity to paclitaxel than the control cells ($P < 0.01$; Fig. 3d).

Discussion

In the present study, we demonstrated that high STMN1 expression is associated with poor prognosis in primary EHCC samples. Moreover, high STMN1 expression is related to low nuclear p27 expression and high cytoplasmic p27 expression. In the *in vitro STMN1* knockdown analysis, proliferative ability was reduced and paclitaxel sensitivity was increased in transfected cells compared with the control cells. In addition, *STMN1* knockdown increased p27 expression.

In the immunohistochemical analysis, high STMN1 expression correlated to poor RFS and CSS prognosis. Moreover, based on the multivariate analysis of CSS, high STMN1 expression translated into an independent prognostic factor. Some reports have also revealed that high STMN1 expression is related to poor prognosis in the following cancers: oral squamous cell carcinoma;[13] diffuse type gastric cancer;[9] colon cancer;[14] hepatocellular cancer;[12] and urothelial carcinoma.[17] The results of the present study are in agreement with these previous reports. Therefore, STMN1 is expected to serve as a prognostic-predictive marker of EHCC.

In the present study, high STMN1 expression was associated with venous invasion in EHCC. Jeon *et al.*[9] reported this association in diffuse type gastric carcinoma and showed that *in vitro* STMN1 suppression inhibited migration and invasion in gastric cancer cells. Baldassare *et al.*[18] reported that STMN1 promotes invasion in sarcoma and regulates microtubule stability following adhesion to the extracellular matrix. STMN1 also regulated invasion in hepatocellular carcinoma.[12] Our results were consistent with these previous reports and indicate that STMN1 is associated with invasion in EHCC.

Previous studies have examined the relationship between STMN1 and p27.[24,25] Baldassarre *et al.*[18] reported that STMN1 bound to p27 in the cytoplasm of sarcoma cells and that high-STMN1-expressing and low-p27-expressing cells demonstrate increased proliferation and invasion ability. However, the authors did not describe in detail whether cytoplasmic p27 regulates STMN1 function or whether cytoplasmic STMN1 inhibits the import of p27 into the nucleus. In our immunohistochemical analysis of EHCC, high-STMN1-expressing samples exhibited a significant tendency for low nuclear p27 expression and high cytoplasmic p27 expression. Using a PLA assay, STMN1 was

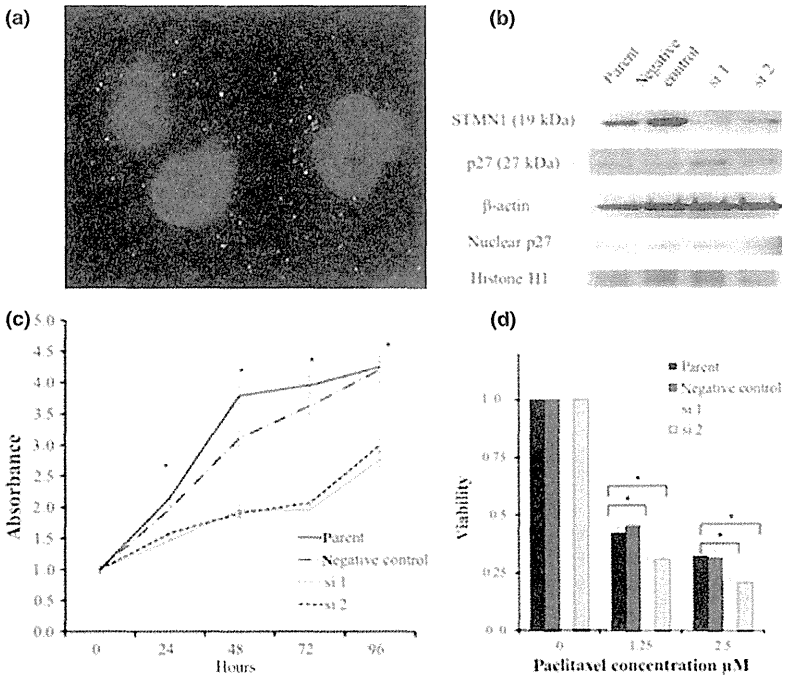

Fig. 3. (a) Stathmin1 (STMN1) bound to p27 in the cytoplasm of HuCCT1 cells. Primary STMN1 rabbit and p27 mouse antibodies bound to STMN1 and p27 complexes were combined with secondary proximity ligation assay probes. The interaction events are visible as red dots (nuclear staining with DAPI). (b) siRNA-mediated STMN1 suppression. STMN1 protein levels were measured using western blotting after transfection with STMN1 siRNA. p27 expression in STMN1 siRNA-transfected and untreated HuCCT-1 cells was assessed using western blotting of total and nuclear protein. β-Actin was used as a loading control for total protein and Histone H1 was used as a loading control for nuclear protein. (c) HuCCT-1 cells were transfected with STMN1 siRNA and WST-8 proliferative assays were performed and compared with untransfected cells. (d) Paclitaxel sensitivity was determined using a WST-8 assay. STMN1 siRNA transfection significantly increased paclitaxel sensitivity compared with untransfected cells. Each time point represents the mean ± SD of triplicate determinations in two independent experiments. $*P < 0.05$.

shown to interact with p27 directly in the cytoplasm of HuCCT1 cells *in vitro*. Moreover, siRNA-mediated *STMN1* knockdown triggered increased p27 expression and the proliferative ability of STMN1-suppressed cells significantly diminished. Interestingly, p27-degradation promotion has been reported in the cytoplasm but not in the nucleus during the G0–G1 transition. From these results it is suggested that STMN1 interacts with p27 in the cytoplasm, inhibits the function of nuclear p27 via the degradation of cytoplasmic p27 and leads to the progression of cancer. S phase kinase-associated protein 2 (SKP2) promotes p27 degradation via the ubiquitin–proteasome system[26] and p27 upregulation facilitated by a SKP2 inhibitor significantly suppresses the cell cycle and results in lower proliferation potency.[27] Therefore, p27 regulation by STMN1 targeting might provide a promising therapeutic tool for several cancers including EHCC.

Some studies have examined the relationship between STMN1 expression and taxane anticancer drugs. STMN1 overexpression levels are associated with paclitaxel sensitivity in ovarian cancer and breast cancer cells.[6,28] Iancu *et al.*[29] reported that taxol and anti-STMN1 therapy produced a synergistic anticancer effect on a leukemic cell line. Moreover, Alli *et al.*[7] also reported that STMN1 overexpression increases the rate of cell death, decreases microtubule polymerization, which markedly decreases taxane binding, and prevents cells from entering mitosis. In the present study, *STMN1* knockdown increased paclitaxel sensitivity, which is consistent with previous reports. Although few anti-microtubule cancer drugs have produced a positive effect on EHCC in current clinical practice, the combination of taxane and anti-STMN1 drugs may provide a prospective therapy against various cancers in the future.

In conclusion, STMN1 expression contributed to a shorter duration of RFS and reduced CSS in patients with EHCC. Therefore, the evaluation of STMN1 expression in EHCC might be a useful predictor of recurrence and poor prognosis. Moreover, high STMN1 expression was associated with low p27 expression in clinical EHCC samples and STMN1 suppression regulated proliferation and paclitaxel sensitivity in an EHCC cell line. Our results suggest that STMN1 in EHCC may be a promising molecular target for controlling cancer progression and taxane resistance via p27 regulation.

Acknowledgments

The authors thank Ms Yukie Saito, Ms Tomoko Yano, Ms Tomoko Ubukata, Ms Yuka Matsui, Ms Ayaka Ishida and Ayaka Ishikubo for their excellent assistance.

Disclosure Statement

The authors have no conflicts of interest.

References

1 Vasilieva LE, Papadhimitriou SI, Dourakis SP. Modern diagnostic approaches to cholangiocarcinoma. *Hepatobiliary Pancreat Dis Int* 2012; **11**: 349–59.
2 Skipworth JR, Olde Damink SW, Imber C, Bridgewater J, Pereira SP, Malago M. Review article: surgical, neo-adjuvant and adjuvant management strategies in biliary tract cancer. *Aliment Pharmacol Ther* 2011; **34**: 1063–78.
3 Pichlmayr R, Weimann A, Klempnauer J *et al.* Surgical treatment in proximal bile duct cancer. A single-center experience. *Ann Surg* 1996; **224**: 628–38.
4 Klempnauer J, Ridder GJ, Werner M, Weimann A, Pichlmayr R. What constitutes long-term survival after surgery for hilar cholangiocarcinoma? *Cancer* 1997; **79**: 26–34.
5 Alli E, Yang JM, Hait WN. Silencing of stathmin induces tumor-suppressor function in breast cancer cell lines harboring mutant p53. *Oncogene* 2007; **26**: 1003–12.

6 Alli E, Yang JM, Ford JM, Hait WN. Reversal of stathmin-mediated resistance to paclitaxel and vinblastine in human breast carcinoma cells. *Mol Pharmacol* 2007; **71**: 1233–40.
7 Alli E, Bash-Babula J, Yang JM, Hait WN. Effect of stathmin on the sensitivity to antimicrotubule drugs in human breast cancer. *Cancer Res* 2002; **62**: 6864–9.
8 Ghosh R, Gu G, Tillman E *et al.* Increased expression and differential phosphorylation of stathmin may promote prostate cancer progression. *Prostate* 2007; **67**: 1038–52.
9 Jeon TY, Han ME, Lee YW *et al.* Overexpression of stathmin1 in the diffuse type of gastric cancer and its roles in proliferation and migration of gastric cancer cells. *Br J Cancer* 2010; **102**: 710–8.
10 Kang W, Tong JH, Chan AW *et al.* Stathmin1 plays oncogenic role and is a target of microRNA-223 in gastric cancer. *PLoS ONE* 2012; **7**: e33919.
11 Singer S, Ehemann V, Brauckhoff A *et al.* Protumorigenic overexpression of stathmin/Op18 by gain-of-function mutation in p53 in human hepatocarcinogenesis. *Hepatology* 2007; **46**: 759–68.
12 Hsieh SY, Huang SF, Yu MC *et al.* Stathmin1 overexpression associated with polyploidy, tumor-cell invasion, early recurrence, and poor prognosis in human hepatoma. *Mol Carcinog* 2010; **49**: 476–87.
13 Kouzu Y, Uzawa K, Koike H *et al.* Overexpression of stathmin in oral squamous-cell carcinoma: correlation with tumour progression and poor prognosis. *Br J Cancer* 2006; **94**: 717–23.
14 Zheng P, Liu YX, Chen L *et al.* Stathmin, a new target of PRL-3 identified by proteomic methods, plays a key role in progression and metastasis of colorectal cancer. *J Proteome Res* 2010; **9**: 4897–905.
15 Ogino S, Nosho K, Baba Y *et al.* A cohort study of STMN1 expression in colorectal cancer: body mass index and prognosis. *Am J Gastroenterol* 2009; **104**: 2047–56.
16 Kim JY, Harvard C, You L *et al.* Stathmin is overexpressed in malignant mesothelioma. *Anticancer Res* 2007; **27**: 39–44.
17 Lin WC, Chen SC, Hu FC *et al.* Expression of stathmin in localized upper urinary tract urothelial carcinoma: correlations with prognosis. *Urology* 2009; **74**: 1264–9.
18 Baldassarre G, Belletti B, Nicoloso MS *et al.* p27(Kip1)-stathmin interaction influences sarcoma cell migration and invasion. *Cancer Cell* 2005; **7**: 51–63.
19 Nakayama K, Ishida N, Shirane M *et al.* Mice lacking p27(Kip1) display increased body size, multiple organ hyperplasia, retinal dysplasia, and pituitary tumors. *Cell* 1996; **85**: 707–20.
20 Denicourt C, Dowdy SF. Cip/Kip proteins: more than just CDKs inhibitors. *Genes Dev* 2004; **18**: 851–5.
21 Sobin LH, Gospodarowicz MK, Wittekind C, eds. *TMN Classification of Malignant Tumors*, 7th edn. Washington, DC. Wiley-Blackwell, 2009.
22 Altan B, Yokobori T, Mochiki E *et al.* Nuclear karyopherin-alpha2 expression in primary lesions and metastatic lymph nodes was associated with poor prognosis and progression in gastric cancer. *Carcinogenesis* 2013; **34**: 2314–21.
23 Suzuki S, Miyazaki T, Tanaka N *et al.* Prognostic significance of CD151 expression in esophageal squamous cell carcinoma with aggressive cell proliferation and invasiveness. *Ann Surg Oncol* 2011; **18**: 888–93.
24 Iancu-Rubin C, Atweh GF. p27(Kip1) and stathmin share the stage for the first time. *Trends Cell Biol* 2005; **15**: 346–8.
25 Karst AM, Levanon K, Duraisamy S *et al.* Stathmin 1, a marker of PI3K pathway activation and regulator of microtubule dynamics, is expressed in early pelvic serous carcinomas. *Gynecol Oncol* 2011; **123**: 5–12.
26 Hara T, Kamura T, Nakayama K, Oshikawa K, Hatakeyama S. Degradation of p27(Kip1) at the G(0)–G(1) transition mediated by a Skp2-independent ubiquitination pathway. *J Biol Chem* 2001; **276**: 48937–43.
27 Wu L, Grigoryan AV, Li Y, Hao B, Pagano M, Cardozo TJ. Specific small molecule inhibitors of Skp2-mediated p27 degradation. *Chem Biol* 2012; **19**: 1515–24.
28 Balachandran R, Welsh MJ, Day BW. Altered levels and regulation of stathmin in paclitaxel-resistant ovarian cancer cells. *Oncogene* 2003; **22**: 8924–30.
29 Iancu C, Mistry SJ, Arkin S, Atweh GF. Taxol and anti-stathmin therapy: a synergistic combination that targets the mitotic spindle. *Cancer Res* 2000; **60**: 3537–41.

Supporting Information

Additional supporting information may be found in the online version of this article:

Fig. S1. Immunohistochemical staining of stathmin1 (STMN1) in primary esophageal cancer served as a positive control.

Fig. S2. Immunohistochemical staining of nuclear p27 in primary esophageal cancer served as a positive control.

Fig. S3. Immunohistochemical staining of cytoplasmic p27 in primary esophageal cancer served as a positive control.

Table S1. Criteria of Immunohisochemistry evaluation.

World J Surg
DOI 10.1007/s00268-014-2488-0

World Journal of Surgery

Extracapsular Lymph Node Involvement is Associated With Colorectal Liver Metastases and Impact Outcome After Hepatectomy for Colorectal Metastases

Hideki Suzuki · Takaaki Fujii · Takayuki Asao · Soichi Tsutsumi · Satoshi Wada · Kenichiro Araki · Norio Kubo · Akira Watanabe · Mariko Tsukagoshi · Hiroyuki Kuwano

Abstract

Background Hepatic resection of metastatic colorectal cancer (CRC) has become the treatment of choice for patients after resection of the primary CRC. However, some patients do not benefit from immediate resection because of rapidly progressive disease. The aim of this study was to examine the prognostic value of extracapsular invasion (ECI) of lymph node (LN) metastasis of CRC with liver metastases following liver resection.

Methods All patients who underwent resection for CRC with liver metastases between 1995 and 2011 were reviewed. All of those with metastasis from primary CRC were included in this study. Preoperative, intraoperative, and postoperative data, including primary tumor pathology results, were retrospectively reviewed. All resected LNs from primary CRC were re-examined to assess ECI. Associations between clinicopathologic factors, survival, and the nodal findings were evaluated.

Results ECI was identified in 47 (48 %) patients. ECI was correlated with the number of positive LNs ($p = 0.0022$), timing of liver metastasis ($p = 0.0238$), and number of liver metastases ($p = 0.0001$). Univariate analysis indicated that the number of positive LNs ($p = 0.0014$), ECI ($p = 0.0203$), and adjuvant chemotherapy ($p = 0.0423$) were significant prognostic factors. Patients with ECI had a significantly worse survival ($p = 0.0024$) after liver resection than patients with LN-negative and ECI-negative groups.

Conclusions In patients with hepatic CRC metastases, ECI in regional LNs reflects a particularly aggressive behavior, such as a greater number of liver metastases. In CRC patients with liver metastases, ECI in regional LNs might be correlated with poor prognosis following liver resection.

H. Suzuki (✉) · T. Fujii · T. Asao · S. Tsutsumi · S. Wada · K. Araki · N. Kubo · A. Watanabe · M. Tsukagoshi · H. Kuwano
Department of General Surgical Science (Surgery I), Gunma University Graduate School of Medicine, Gunma University, 3-39-22 Showa-machi, Maebashi 371-8511, Japan
e-mail: hsuzuki044@gunma-u.ac.jp

Introduction

In selected patients, liver metastases may be amenable to surgical resection, with 5-year survival rates of 35–40 % [1–3]. For those with unresectable liver metastases or who experience recurrence after resection, the prognosis is poor. With improvements in systemic and regional chemotherapy and in surgical technique and perioperative care, indications for hepatectomy have expanded to include patients with large lesions and multiple or bilobar lesions. However, some patients do not benefit from immediate resection because of rapidly progressive disease or micrometastases that lead to early recurrence. Therefore, careful patient selection is mandatory for achieving good outcomes.

Some authors have proposed waiting several months before liver resection so as to assess the biologic behavior of the neoplasm, to treat potentially occult disease, and to avoid operating on patients with rapidly progressing tumors [4–6]. Some authors performed neoadjuvant chemotherapy to see the patients' response, insisting that such response is an important prognostic factor for patients with multiple and bilobar liver metastases [7–9].

Numerous prognostic parameters after resection of liver metastases have been described. These studies were

Published online: 11 March 2014

designed to identify factors that should be considered contraindications to liver resection, to identify patients who might benefit from liver resection, or to estimate the risk of recurrence after liver surgery [10–15]. Those studies attempted to examine prognostic factors for tumor recurrence after resection. However, data are not easily generalized and are mainly representative of a single center's experience, which may be biased by indications and surgical technique.

Histologic findings of lymph node (LN) metastases comprise one prognostic indicator for patients with metastatic colorectal cancer (CRC). Numerous reports have assessed the correlation between the histology of LN metastasis and prognosis in patients undergoing hepatic resection [12, 16, 17]. Some studies reported that an increase in the number of metastatic regional LNs was associated with a worse outcome [18, 19]. More recently, disease-specific survival and recurrence rates were found to be statistically significantly influenced by metastases of the primary tumor to more than three LNs [15].

Extracapsular invasion (ECI) by LN metastasis has been studied for several malignancies, including breast, prostate, and lung cancer [20–22]. ECI in LN metastases is extension of cancer cells through the nodal capsule and into the perinodal fatty tissue. The presence of ECI in LN metastasis at the N1 site is correlated with further metastasis at the N2 site and might be a significant prognostic factor in patients with CRC [23].

At present, it is unclear whether the clinical behavior of patients with ECI is similar to that of patients with no ECI in patients with CRC liver metastases. The ability of nodal metastases to permit the tumor to break down the LN capsule represents very aggressive CRC biology. It is possible that these aggressive biologic features influence liver metastases. In the present study, we evaluated the incidence of ECI in LN metastases from primary CRCs. We also assessed the prognostic significance of ECI in patients after hepatectomy for CRC liver metastases.

Materials and methods

Patients

Patients who had undergone resection for CRC with liver metastases were identified from the clinical histopathology database at the Department of General Surgical Science, Graduate School of Medicine, Gunma University, from January 1995 until December 2011. All patients with LN involvement were included in the present study. Patients with no regional LN metastases from a primary CRC were defined as the negative controls. Patients with inflammatory bowel disease or familial adenomatous polyposis and those who had undergone preoperative chemoradiotherapy before primary tumor resection were excluded. Data examined included age, sex, primary tumor site, pathology of the primary CRC, ECI at the metastatic LN involvement from the primary tumor, presentation of liver metastases, extent of liver lesions, surgical details of the liver resection, timing of hepatic metastases, number of tumors, and largest tumor size of the liver metastases. Each liver lesion that was present concomitantly with the primary CRC was considered a synchronous metastasis. Each liver metastasis diagnosed after CRC resection was considered a metachronous metastasis. The metachronous liver metastases were further divided into two groups: an early group and a late group. The early group includes patients who showed liver metastases within 2 years after CRC resection. The late group includes patients who showed liver metastases more than 2 years after CRC resection.

Hepatectomy

Fitness for liver surgery was assumed by survival from colorectal resection and a willingness to proceed regardless of age. The presence of extrahepatic metastases other than resectable lung metastases was considered a relative contraindication to hepatectomy. The indication for liver resection was complete removal of the liver metastasis if complete resection of the lesions could be accomplished while saving 30 % of the total liver volume. The resectability of liver lesions was evaluated by means of contrast-enhanced computed tomography (CT) and/or magnetic resonance imaging (MRI) and positron emission tomography. Liver function was assessed using indocyanine green retention at 15 min and/or technetium-99 m galactosyl serum albumin scintigraphy. All patients underwent intraoperative ultrasonography to complement the visual exploration. The type of surgical procedure employed was selected based on the extent of the tumor and the potential for preserving hepatic function. The extent of the resection was defined as major when more than three segments were resected. Treatment with chemotherapy was recorded as preoperative (no more than 6 months before liver resection) or adjuvant (after liver resection). The applied protocols were either oxaliplatin-based (FOLFOX) or 5-fluorouracil (5-FU)/leucovorin.

Histopathology

After resection, the pathologist who examined the operative specimen carefully palpated the specimen, and all palpable LNs were collected and evaluated. Routine hematoxylin and eosin (H&E) staining was performed using a standardized protocol. Extracapsular LN involvement was defined as invasive cancer showing penetration at

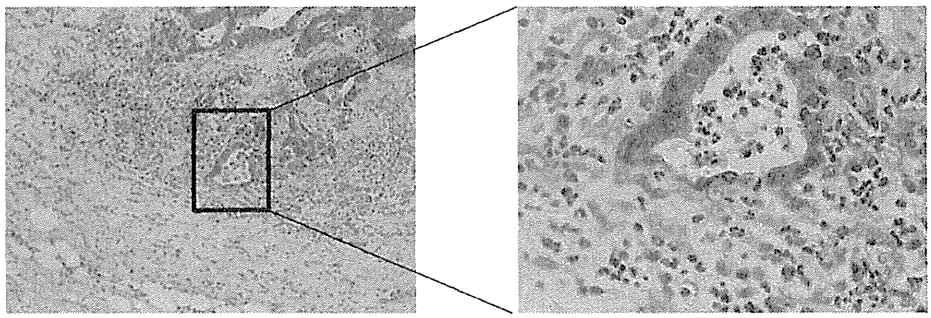

Fig. 1 Lymph node (LN) with a metastatic lesion. Cancer cells are penetrating the LN capsule and infiltrating the perinodal adipose tissue

least of the nodal capsule or extending through the nodal capsule into the perinodal adipose tissue (Fig. 1).

Patient follow-up

Postoperative patient follow-up was continued at the outpatient clinic every 2 months for the first 3 years and then every 3 months for the subsequent 2 years. The patients were checked by physical examination and assessed for serum levels of the tumor markers carcinoembryonic antigen (CEA) and carbohydrate antigen at each visit. CT scanning was performed every year. When liver metastases were highly suspected, the patients underwent gadolinium ethoxybenzyl-diethylenetriamine pentaacetic acid MRI to detect small liver metastases.

Statistical methods

Statistical computations were performed using JMP software (SAS Institute, Cary, NC, USA). Continuous variables were expressed as medians and were compared using the Wilcoxon test, whereas categoric variables were compared using Fisher's exact test or the χ^2 test. Univariate analyses were performed by Cox proportional hazards regression. Multivariate logistic regression was performed by including factors with a value of $p < 0.05$ in the univariate analysis. Survival curves were calculated by the Kaplan–Meier method. The log-rank test was used to assess differences in survival. Statistical significance was defined as $p < 0.05$. For disease-specific survival, only deaths attributable to recurrent cancer were considered events. Patients who died from secondary causes without recurrence were treated as censored.

Results

Patients

Between January 1995 and December 2011, a total of 121 patients with liver metastasis from colorectal

Table 1 Clinicopathologic characteristics (LN-positive)

Variable	No.	%
Sex		
Male	51	52.6
Female	46	47.4
Age (years): mean and range	62 (31–83)	
Primary site		
Colon	67	69.7
Rectum	30	30.9
pT		
pT2	3	3.1
pT3	57	58.8
pT4	37	38.1
No. of positive LNs (range)	2.9 ± 2.1 (1–10)	
ECI		
Positive	47	48.5
Negative	50	51.5
Histology		
Well differentiated	12	12.4
Moderately differentiated	68	70.1
Poorly differentiated/mucinous	7	7.2
Lymphovascular invasion		
Negative	31	32.0
Positive	66	68.0
Timing of development		
Metachronous	22	22.9
Synchronous	75	77.3
No. of metastases		
1–2	46	47.4
≥3	51	52.6
Maximum diameter (cm)		
<3	55	56.7
≥3	42	43.3
Tumor distribution		
Unilateral	49	50.5
Bilateral	48	49.5

LNs lymph nodes, *ECI* extracapsular invasion